Stem Cell Reports
Article

ISSCR

OPEN ACCESS

The *miR-590/Acvr2a/Terf1* Axis Regulates Telomere Elongation and Pluripotency of Mouse iPSCs

Qidong Liu,[1,2] Guiying Wang,[1,2] Yao Lyu,[1] Mingliang Bai,[1] Zeyidan Jiapaer,[1] Wenwen Jia,[1] Tong Han,[1] Rong Weng,[1] Yiwei Yang,[1] Yangyang Yu,[1] and Jiuhong Kang[1,*]

[1]Clinical and Translational Research Center of Shanghai First Maternity and Infant Health Hospital, Shanghai Key Laboratory of Signaling and Disease Research, Collaborative Innovation Center for Brain Science, School of Life Sciences and Technology, Tongji University, 1239 Siping Road, Shanghai 200092, People's Republic of China

[2]Co-first author

*Correspondence: jhkang@tongji.edu.cn

https://doi.org/10.1016/j.stemcr.2018.05.008

SUMMARY

During reprogramming, telomere re-elongation is important for pluripotency acquisition and ensures the high quality of induced pluripotent stem cells (iPSCs), but the regulatory mechanism remains largely unknown. Our study showed that fully reprogrammed mature iPSCs or mouse embryonic stem cells expressed higher levels of *miR-590-3p* and *miR-590-5p* than pre-iPSCs. Ectopic expression of either *miR-590-3p* or *miR-590-5p* in pre-iPSCs improved telomere elongation and pluripotency. *Activin receptor II A* (*Acvr2a*) is the downstream target and mediates the function of *miR-590*. Downregulation of *Acvr2a* promoted telomere elongation and pluripotency. Overexpression of *miR-590* or inhibition of ACTIVIN signaling increased *telomeric repeat binding factor 1* (*Terf1*) expression. The p-SMAD2 showed increased binding to the *Terf1* promoter in pre-iPSCs compared with mature iPSCs. Downregulation of *Terf1* blocked *miR-590*- or sh*Acvr2a*-mediated promotion of telomere elongation and pluripotency in pre-iPSCs. This study elucidated the role of the *miR-590/Acvr2a/Terf1* signaling pathway in modulating telomere elongation and pluripotency in pre-iPSCs.

INTRODUCTION

During reprogramming, the inefficient induction and low quality of induced pluripotent stem cells (iPSCs) with abnormal gene expression and chromosome integrity limit potential applications for future clinical therapy (Jiang et al., 2013; Pera, 2011). The telomere is re-elongated after sperm-oocyte binding (Liu et al., 2007). Telomerase activity is high in iPSCs (Takahashi and Yamanaka, 2006). The efficiency of chimera generation of iPSCs is higher in cells with longer telomeres than those with short telomeres. Moreover, embryonic stem cells (ESCs) with short telomeres also show reduced teratoma formation and chimera production (Huang et al., 2011). Previous study showed that the reprogramming efficiency of iPSCs derived from mouse embryonic fibroblasts (MEFs) of telomerase gene $Terc^{-/-}$ mice was decreased (Marion et al., 2009). Mouse iPSCs with short telomeres show a lower capacity for teratoma formation or chimera production, failing to generate complete pups (Zhao et al., 2009). During reprogramming, the re-elongation of telomeres is thus critically important for pluripotency acquisition.

Lengthening of telomeres in iPSCs induced with four factors (*Oct4*, *Sox2*, *c-Myc*, and *Klf4*) is dependent on telomerase activity and is a very slow process, involving several passages after reprogramming to reach similar lengths to ESC telomeres (Marion et al., 2009). By contrast, telomere lengths quickly and extensively increase during somatic cell nuclear transfer (SCNT) reprogramming (Lanza et al., 2000; Wakayama et al., 2000). Oocytes contain sufficient factors for efficient high-quality somatic reprogramming using SCNT compared with the limited factors in the induction of iPSCs (Brambrink et al., 2006; Wakayama et al., 2006; Yang et al., 2007). The overexpression of *Zscan4*, an oocyte-related factor, during iPSC induction significantly improved telomere elongation and increased reprogramming efficiency and pluripotency through the telomerase-independent alternative lengthening of telomeres (ALT) (Jiang et al., 2013; Lee and Gollahon, 2015). In addition, the protein complex Shelterin, which contains TERF1, TERF2, POT1, RAP1, TIN2, and TPP1 (Xin et al., 2008), was also important for telomere length and stabilization. *Terf1* has been reported to play a key role in both telomerase-dependent telomere maintenance and the ALT process (Ho et al., 2016). TERF1 co-localizes and interacts indirectly with ZSCAN4 in the cell nucleus (Lee and Gollahon, 2015). TERF1, along with TERF2, normally prevents telomerase from adding more telomere units to telomeres to balance the telomere length (Diotti and Loayza, 2011). However, when telomere lengthening is required, TERF1 recruits helicases to facilitate the process (Sfeir, 2012). In addition, *Terf1* is highly expressed in ESCs and iPSCs as a stemness marker (Boue et al., 2010; Schneider et al., 2013). However, whether *Terf1* participates in the regulation of reprogramming telomere re-elongation remains unknown.

Pre-iPSCs, the partially reprogrammed cells, provide a useful model for studying the regulatory mechanism of reprogramming. Pre-iPSCs exhibit ESC-like morphology but show low pluripotency and cannot form chimeras (Silva et al., 2008; Wei et al., 2015). Pre-iPSCs could be activated to naive pluripotency cells by inhibitor of mitogen-activated protein kinase (MAPK, PD0325901) and inhibitor of glycogen synthase kinase 3 beta (GSK3B, CHIR99021) with the leukemia inhibitory factor (LIF) culture (Theunissen et al., 2011). Knockdown of *Hdac2* promotes the four factors that induce iPSC generation and also converts pre-iPSCs into the fully reprogrammed state (Wei et al., 2015). The pre-iPSCs can also be a valuable resource for investigating telomere regulation during iPSC induction.

Recently, a group of microRNAs (miRNAs) were connected to the transcriptional regulatory circuitry of telomere length modulation and pluripotency during the reprogramming of iPSCs. The overexpression of *miR-302/367* inhibited the expression of *Hdac2* to promote efficient iPSC induction (Anokye-Danso et al., 2011). The *miR-17∼92*, *miR-106b∼25*, and *miR-106a∼363* clusters were highly expressed and inhibited the expression of *transforming growth factor beta receptor 2* (*Tgfbr2*) to promote reprogramming (Li et al., 2011). *MiR-23a* repressed the expression of *Terf2*, resulting in abnormal telomere function (Luo et al., 2015). *MiR-155* directly targeted *Terf1* to induce telomere fragility (Dinami et al., 2014). However, whether miRNAs can regulate telomere-related genes and increase pluripotency during iPSC induction remains largely unknown.

Transforming growth factor beta (TGFB) family genes were reported to inhibit *Tert* expression via the regulation of SMAD3 phosphorylation (Cassar et al., 2010). BMP7 induced telomere shortening in breast cancer cells (Cassar et al., 2009). The inhibition of signaling substituted for *Oct4* during iPSC induction and maintained pluripotency (Tan et al., 2015). The inhibition of TGFB also promoted the expression of *Nanog* (Ichida et al., 2009). In addition, the repression of NODAL/ACTIVIN signaling mediated the function of Polycomb in increasing the reprogramming efficiency (Dahle and Kuehn, 2013). However, whether TGFB family-related signaling influences telomere elongation and pluripotency of iPSCs during cell reprogramming remains unclear.

Our study showed that *miR-590-3p* and *miR-590-5p* in mature iPSCs and ESCs had increased expression compared with pre-iPSCs. The ectopic expression of *miR-590-3p* and *miR-590-5p* promoted the telomere elongation and pluripotency of pre-iPSCs. We further found that both *miR-590-3p* and *miR-590-5p* upregulated *Terf1* expression by targeting *Activin receptor II A* (*Acvr2a*). This work elucidated the role of the *miR-590/Acvr2a/Terf1* signaling pathway in modulating pluripotency and telomere elongation in pre-iPSCs.

RESULTS

miR-590 Is Highly Expressed in Fully Pluripotent Cells and Promotes Telomere Elongation and Pluripotency in Pre-iPSCs

To observe the difference in quality among pre-iPSCs, mature iPSCs, and ESCs, we detected stemness marker expression levels and differentiated these cells into three germ layers. Compared with ESCs and mature iPSCs, pre-iPSCs showed lower expression levels of stemness markers *Oct4*, *Sox2*, *Nanog*, and *Esrrb* (Figure 1A). In addition, the pre-iPSC cell line used for this research was established in our laboratory for previous study and failed at maturation process (Wei et al., 2015). The immunofluorescence staining indicated that SOX2 and SSEA1 were significantly lower in pre-iPSCs than in mature iPSCs and ESCs (Figure S1A). The expression level of *Nanog*, *Esrrb*, *Rex1*, *Cripto*, and *Sall4* (Figures 1A and S1B) also confirmed the maturation of iPSCs (Wei et al., 2015). The differentiation potentials to the three germ layers were also decreased in pre-iPSCs (Figures 1B and S1C). The telomere length of pre-iPSCs cells was significantly shorter than that of the ESCs and mature iPSCs (Figures 1C and 1D). The expression levels of *miR-590-3p* and *miR-590-5p* were higher in mature iPSCs and ESCs than in pre-iPSCs (Figure 1E). Then, we enhanced the pre-iPSC maturation by adding the 2i compounds (1 μM PD0325901 and 3 μM CHIR99021) into the medium and found that the stemness markers were upregulated (Figure 1F) with the telomere elongation (Figure 1G) during 1 week in pre-iPSCs. We transfected the *miR-590-3p* and *miR-590-5p* inhibitors in the pre-iPSCs and found that inhibition of *miR-590* repressed the pluripotency acquisition of pre-iPSCs treated by 2i (Figure S1D). However, the expression of *Gsk3b* related to the CHIR99021 and *Map2k1* related to the PD0325901 were not significantly changed in the pre-iPSCs transfected with *miR-590-5p* and *miR-590-3p* inhibitors (Figure S1E). Overexpression of *Oct4* could increase the expression level of *miR-590-3p* and *miR-590-5p* (Figure S1F). Our previous study indicated the inhibition of *miR-590* could increase the proliferation of ESCs (Liu et al., 2014). We also confirmed the inhibition of *miR-590* promoted the proliferation of mature iPSCs (Figure S1G). Knockdown of *Rad51b*, the downstream target of *miR-590* (Liu et al., 2014), could also increase the proliferation of mature iPSCs (Figure S1H) but had no significant effect on pluripotency (Figure S1I). During the maturation process of pre-iPSCs, the expression level of *miR-590* was also upregulated (Figure 1H). Overexpression of *miR-590-3p* or *miR-590-5p* in pre-iPSCs promoted the re-elongation of

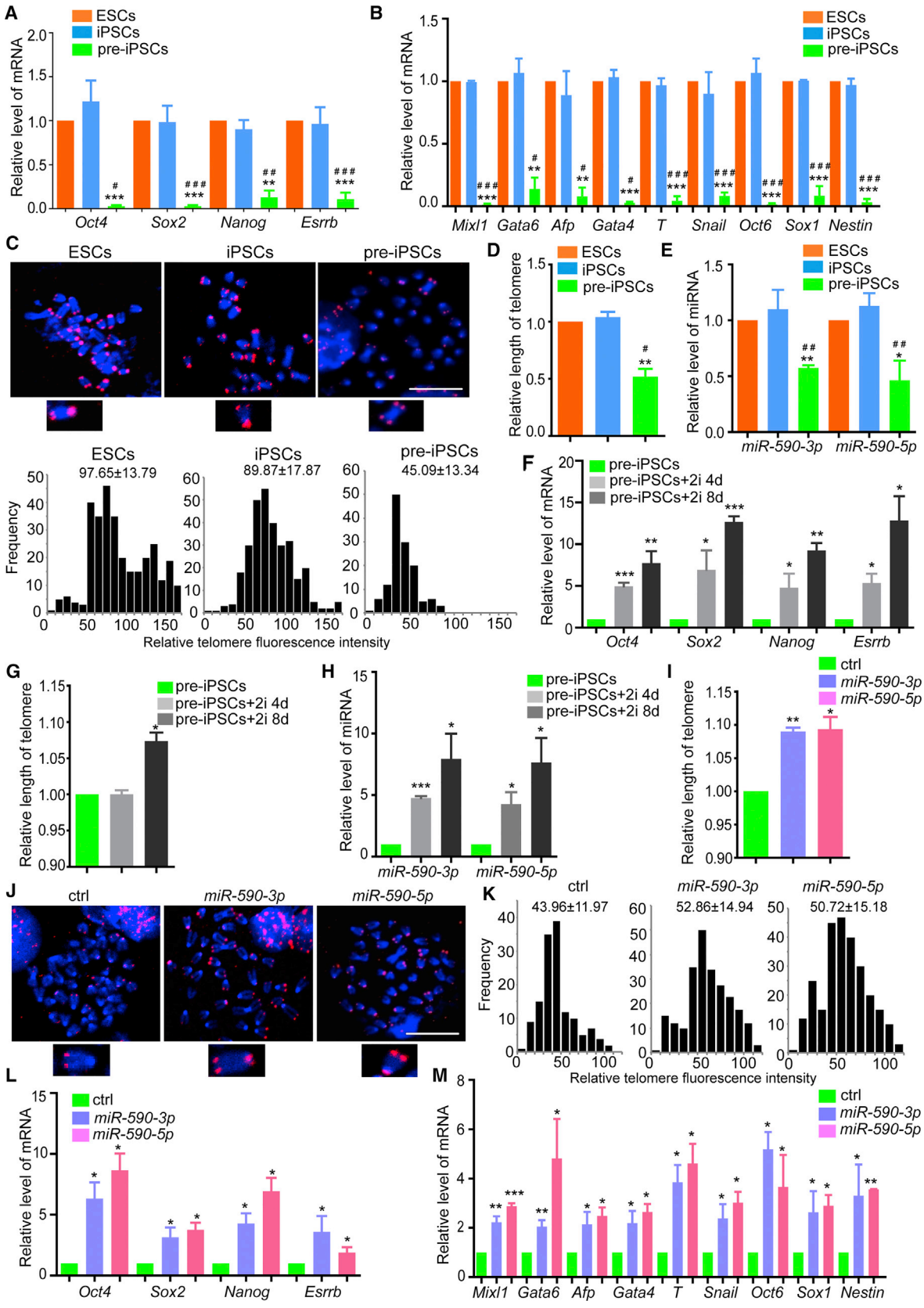

(legend on next page)

telomere length compared with the control group (Figures 1I–1K). Pluripotency was also increased by overexpressing *miR-590* (Figures 1L and 1M).

Inhibition of *Acvr2a* Improves Telomere Re-elongation to Promote Pluripotency in Pre-iPSCs

Our previous study identified *Acvr2a* as a downstream target of *miR-590-3p* and *miR-590-5p* (Liu et al., 2014). Here, we found that *Acvr2a* expression was downregulated in pre-iPSCs overexpressing *miR-590* (Figure 2A). Then, knockdown of *Acvr2a* in pre-iPSCs (Figure 2B) showed that the telomeres could be elongated (Figures 2C and 2D). The expression level of stemness markers (Figures 2E and S2A) and the differentiation potentials to the three germ layers were both increased after knockdown of *Acvr2a* (Figures 2F and S2B).

The *miR-590/Acvr2a* Pathway Modulates Telomere Length and the Pluripotency of Pre-iPSCs

To determine whether *Acvr2a* mediated the function of *miR-590* in regulating telomeres and pluripotency in pre-iPSCs, we performed rescue experiments and found that the overexpression of *Acvr2a* significantly blocked the promotion of telomere re-elongation by *miR-590-3p* overexpression (Figures 3A and 3B). The expression levels of stemness markers (Figures 3C and S3A) and three germ layer markers (Figures 3D and S3B) were blocked by *Acvr2a* overexpression. Furthermore, we co-overexpressed *Acvr2a* with *miR-590-5p* and found that *Acvr2a* could block the telomere re-elongation promoted by *miR-590-5p* overexpression (Figures 3E and 3F). The expression levels of stemness markers (Figures 3G and S3A) and three germ layer markers (Figures 3H and S3C) were also blocked by *Acvr2a* overexpression.

Terf1 Is Critically Involved in Modulating Pre-iPSC Telomere Length and Pluripotency

We performed differential expression analysis of telomere-related genes between mature iPSCs and pre-iPSCs and found that *Terf1* was highly expressed in mature iPSCs and was much higher than in pre-iPSCs (Figure 4A). So we hypothesized that *Terf1* might play critical role in regulating pre-iPSCs telomere. Overexpression of either *miR-590-3p* or *miR-590-5p* upregulated *Terf1* in pre-iPSCs (Figure 4B). Furthermore, we found that *Terf1* expression was upregulated during the induction process of iPSCs (Figure 4C). The overexpression of *Terf1* increased telomere length (Figures 4D and 4E). In addition, *Terf1* promoted pluripotency acquisition in pre-iPSCs (Figures 4F, 4G, S4A, and S4B).

Terf1 Mediates the *Acvr2a* Function in Regulating Telomere Elongation and Pluripotency

After the addition of SB431542 (50 μM), an ACTIVIN signaling inhibitor of p-SMAD2 signaling, into the pre-iPSC culture medium, we found that *Terf1* was upregulated

Figure 1. High Expression of *miR-590* in Fully Pluripotent Cells Promotes Telomere Elongation and Pluripotency in Pre-iPSCs

(A) qRT-PCR showed the low expression of stemness markers *Oct4*, *Sox2*, *Nanog*, and *Esrrb* in mouse pre-iPSCs compared with ESCs and iPSCs. Data shown are the mean ± SD (n = 5).

(B) Detecting markers of three germ layers, including endoderm (*Mixl1*, *Gata6*, and *Afp*), mesoderm (*Gata4*, *T*, and *Snail*), and ectoderm (*Oct6*, *Sox1*, and *Nestin*), derived from mouse ESCs, iPSCs, and pre-iPSCs by qRT-PCR. Data shown are the mean ± SD (n = 3).

(C) Fluorescence *in situ* hybridization (FISH) detection of telomere staining in ESCs, iPSCs, and pre-iPSCs showed the shorter length of telomere in pre-iPSCs. The bottom panel shows the statistics of relative telomere length (relative telomere fluorescence intensity) by histogram measured by FISH. Scale bar indicates 10 μm.

(D) Relative length of telomeres in ESCs, iPSCs, and pre-iPSCs detected by qPCR. Data shown are the mean ± SD (n = 3).

(E) Lower expression of *miR-590-3p* and *miR-590-5p* in pre-iPSCs than in ESCs and iPSCs detected by qRT-PCR. Data shown are the mean ± SD (n = 4).

(F) qRT-PCR detection showed the gradual upregulation of stemness markers by 2i induction in pre-iPSCs on 4 days (4d) and 8 days (8d). Data shown are the mean ± SD (n = 3).

(G) Telomere could elongate in the 2i-treated pre-iPSCs detected by qPCR. Data shown are the mean ± SD (n = 4).

(H) Upregulation of *miR-590-3p* and *miR-590-5p* during the maturation process by 2i treatment. Data shown are the mean ± SD (n = 3).

(I) Both *miR-590-3p* and *miR-590-5p* promoted telomere elongation. Data shown are the mean ± SD (n = 3).

(J) FISH detection of telomere staining showed improvement in telomere elongation by overexpression of *miR-590-3p* or *miR-590-5p*. Scale bar indicates 10 μm.

(K) The statistics of (J).

(L) *MiR-590-3p* or *miR-590-5p* overexpression increased the expression level of stemness markers in pre-iPSCs. Data shown are the mean ± SD (n = 3).

(M) Three germ layer markers were upregulated in the cells derived from the *miR-590-3p* or *miR-590-5p*-overexpressing pre-iPSCs. Data shown are the mean ± SD (n = 3).

For all data, * and $^{\#}p < 0.05$, ** and $^{\#\#}p < 0.01$, *** and $^{\#\#\#}p < 0.001$. In (A), (B), and (D), the asterisk (*) means the significance in the comparison of ESCs group with the pre-iPSCs group; hash (#) means the significance of the statistics of the iPSCs and pre-iPSCs group. In other panels, the asterisk means the significance of the comparison of treated cell group with the control (ctrl) group.

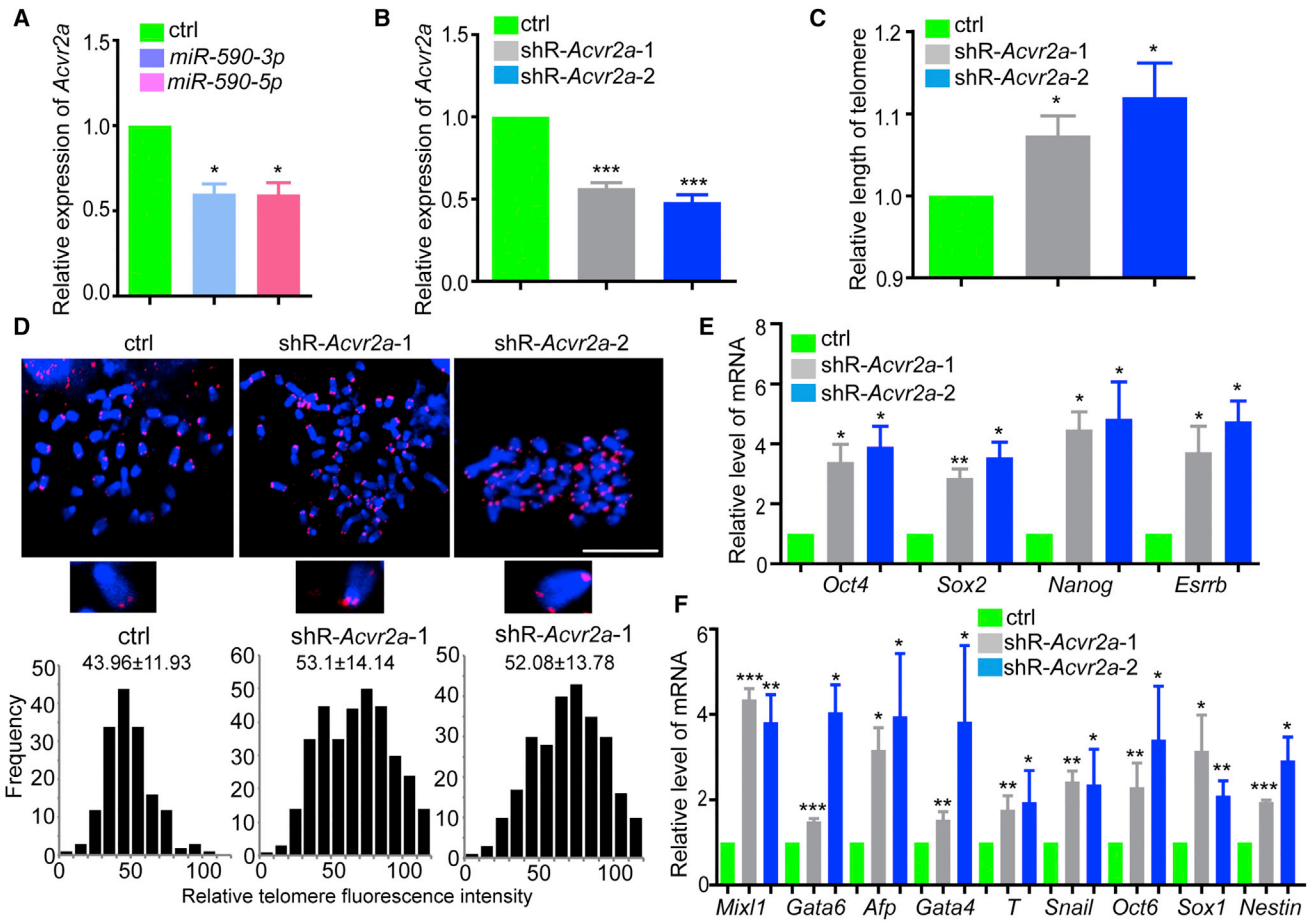

Figure 2. Inhibition of *Acvr2a* Improves Telomere Re-elongation to Promote Pluripotency in Pre-iPSCs

(A) *MiR-590-3p* or *miR-590-5p* downregulated the mRNA level of *Acvr2a* detected by qRT-PCR. Data shown are the mean ± SD (n = 3).

(B) Detecting the efficiency of *Acvr2a* knockdown in pre-iPSCs. Data shown are the mean ± SD (n = 3).

(C) Downregulation of *Acvr2a* promoted telomere elongation. Data shown are the mean ± SD (n = 3).

(D) FISH staining of telomeres and histogram statistics showed the promotion of telomere elongation by downregulating *Acvr2a*. Scale bar indicates 10 μm.

(E) Stemness markers were upregulated in *Acvr2a* knockdown pre-iPSCs. Data shown are the mean ± SD (n = 3).

(F) *Acvr2a* knockdown increased the pluripotency of pre-iPSCs. Data shown are the mean ± SD (n = 3).

For all data, *p < 0.05, **p < 0.01, and ***p < 0.001.

(Figure 5A). Then, we performed chromatin immunoprecipitation (ChIP) assays to assess the binding of p-SMAD2 to the *Terf1* promoter in pre-iPSCs and found that it was increased compared with binding in mature iPSCs (Figure 5B). Inhibition of p-SMAD2 by SB431542 also showed more binding of POL II on *Terf1* promoter (Figure S5A). Knockdown of *Acvr2a* also increased the expression of *Terf1* (Figure 5C). Knockdown of *Terf1* blocked the effect on telomere elongation caused by the downregulation of *Acvr2a* (Figures 5D and 5E). In addition, knockdown of *Terf1* blocked the promoting effect of *Acvr2a* downregulation on pluripotency (Figures 5F, 5G, S5B, and S5C).

Terf1 Is the Functional Downstream Mediator of *miR-590* in Regulating Telomere Elongation and Pluripotency

We performed rescue experiments and found that the downregulation of *Terf1* blocked the *miR-590-3p*-mediated increase in telomere elongation (Figures 6A and 6B). The expression levels of pluripotent genes (Figures 6C and S6A) and three germ layer markers (Figures 6D and S6B) were also blocked by knockdown of *Terf1* in *miR-590-3p*-overexpressing pre-iPSCs. Similarly, downregulation of *Terf1* blocked the re-elongation of telomeres promoted by *miR-590-5p* overexpression (Figures 6E and 6F). Moreover, the expression levels of pluripotent genes (Figures 6G and

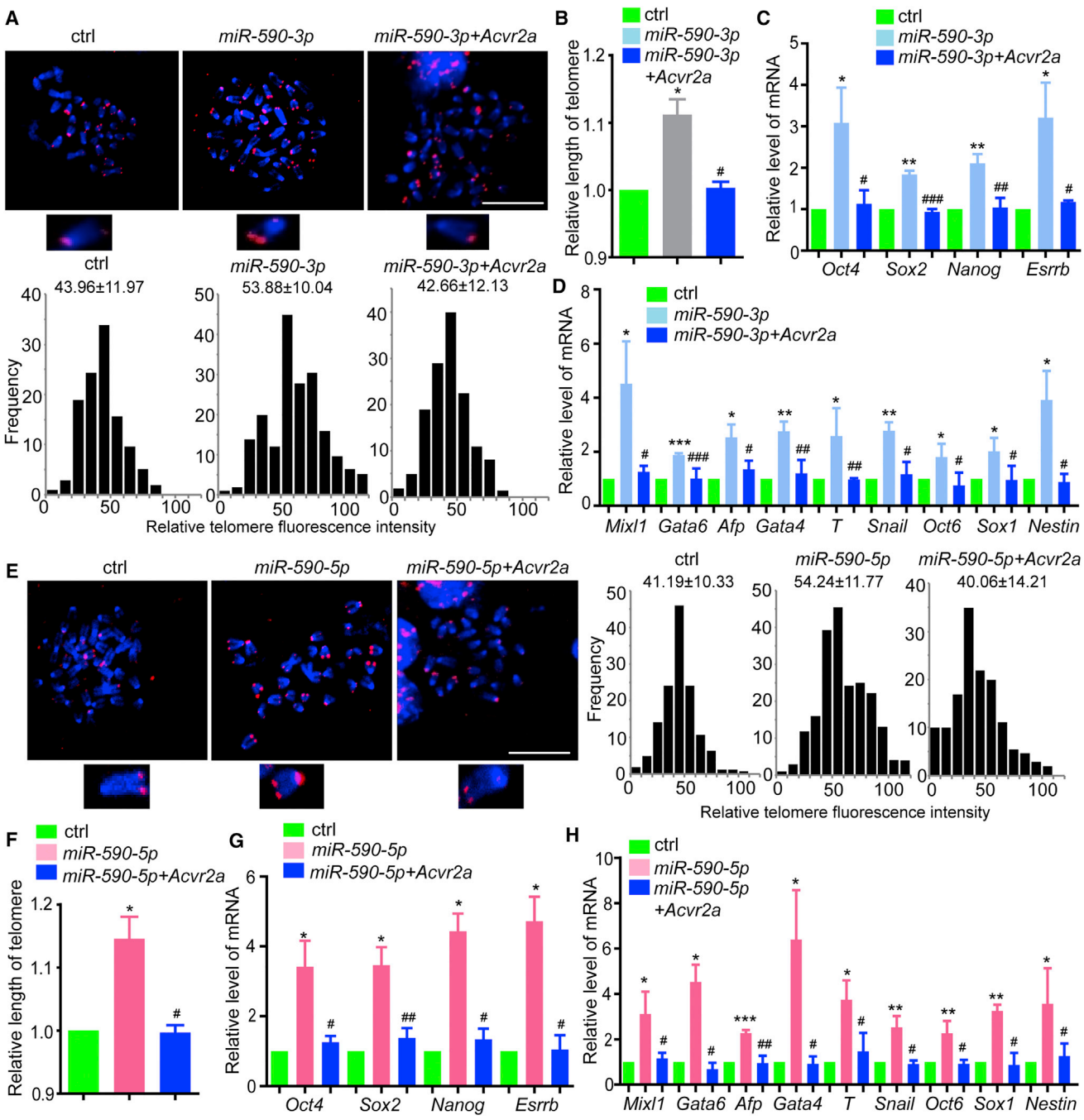

Figure 3. The *miR-590/Acvr2a* Pathway Modulates Telomere Length and the Pluripotency of Pre-iPSCs

(A) Telomere FISH staining and histogram statistics (bottom) showed that the overexpression of *Acvr2a* blocked the function of *miR-590-3p* on regulating telomere elongation in the rescue experiments. Scale bar indicates 10 μm.

(B) Detection of the telomeres by qPCR in the rescue experiment. Data shown are the mean ± SD (n = 3).

(C) *Acvr2a* restored the expression of stemness markers upregulated by *miR-590* to be similar with the control group in the rescue experiment. Data shown are the mean ± SD (n = 3).

(D) *Acvr2a* blocked the increase of pluripotency caused by overexpression of *miR-590-3p* in pre-iPSCs. Data shown are the mean ± SD (n = 3).

(E and F) (E) FISH staining of telomeres and histogram statistics (right) and (F) qPCR detection both showed that *Acvr2a* blocked the *miR-590-5p* function in promoting telomere elongation. Scale bar indicates 10 μm. Data shown are the mean ± SD (n = 3).

(legend continued on next page)

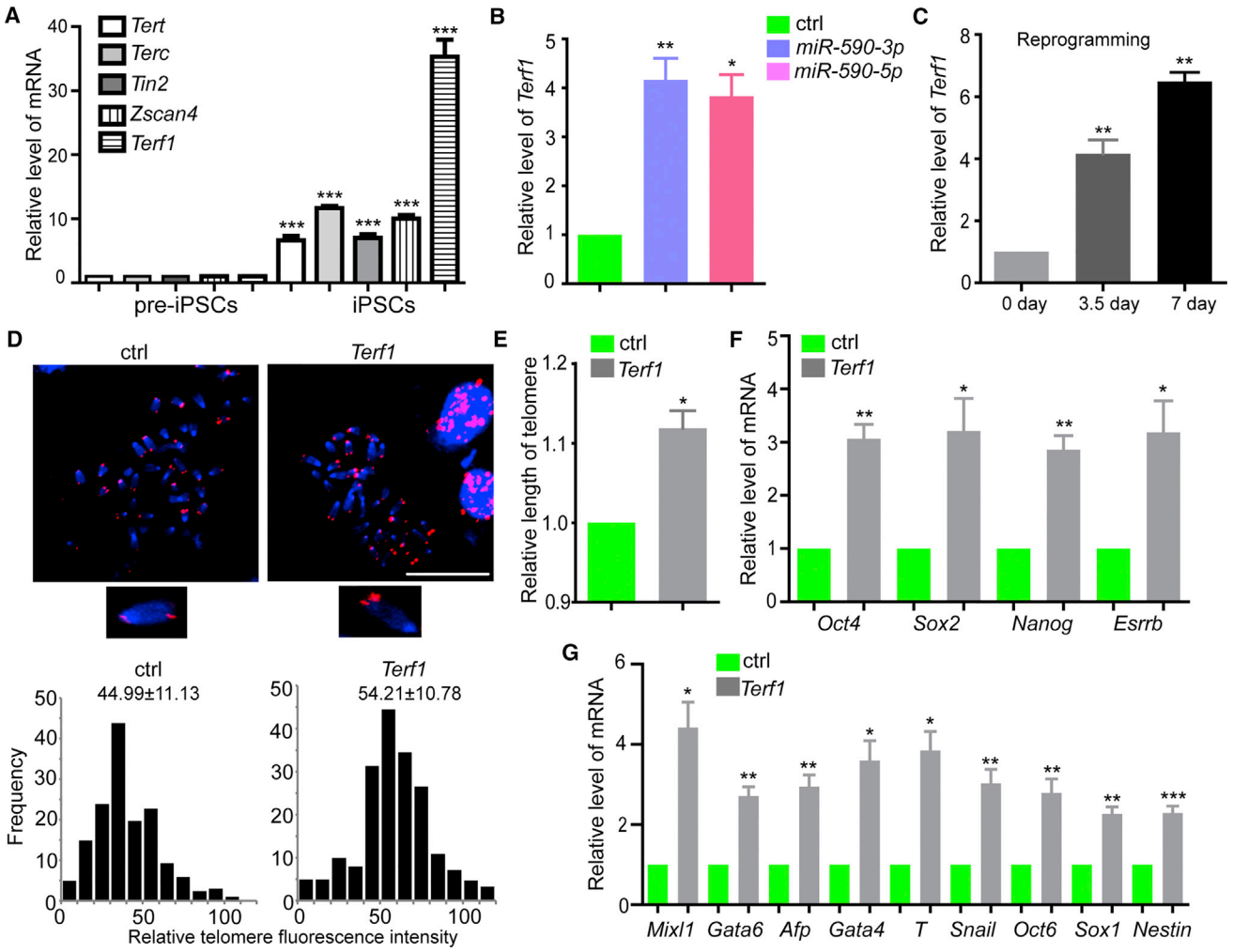

Figure 4. *Terf1* Is Critically Involved in Modulating Pre-iPSC Telomere Length and Pluripotency

(A) Relative expression level of telomere-related genes in iPSCs and pre-iPSCs. The *Terf1* expressed highly in mature iPSCs compared with pre-iPSCs. Data shown are the mean ± SD (n = 3).

(B) *MiR-590* promoted the expression of *Terf1*. Data shown are the mean ± SD (n = 3).

(C) The expression level of *Terf1* was upregulated during cell reprogramming. Data shown are the mean ± SD (n = 3).

(D and E) (D) FISH staining of telomeres and histogram statistics (bottom) and (E) qPCR detection indicated that *Terf1* overexpression improved telomere elongation. Scale bar indicates 10 μm. Data shown are the mean ± SD (n = 3).

(F and G) (F) *Terf1* promoted stemness marker expression and (G) the pluripotency in pre-iPSCs. Data shown are the mean ± SD (n = 3).

For all data, *p < 0.05, **p < 0.01, ***p < 0.001.

S6A) and three germ layer markers (Figures 6H and S6C) were similar to the control groups following the downregulation of *Terf1* with the overexpression of *miR-590-5p* in pre-iPSCs.

DISCUSSION

iPSC induction remains an inefficient process (Stadtfeld and Hochedlinger, 2010). Although studies have suggested

(G and H) (G) Detection of the *Acvr2a* function blocking the promotion of stemness marker expression and (H) the pluripotency of differentiation capacity regulated by *miR-590-5p*. Data shown are the mean ± SD (n = 3).

For all data, * and #p < 0.05, ** and ##p < 0.01, *** and ###p < 0.001. Asterisk (*) means the statistical significance of the *miR-590-5p* and *miR-590-3p* group compared with the control group; hash (#) means the statistical significance of the *miR-590-5p* + *Acvr2a* and *miR-590-3p* + *Acvr2a* group compared with the corresponding *miR-590-5p* and *miR-590-3p* group.

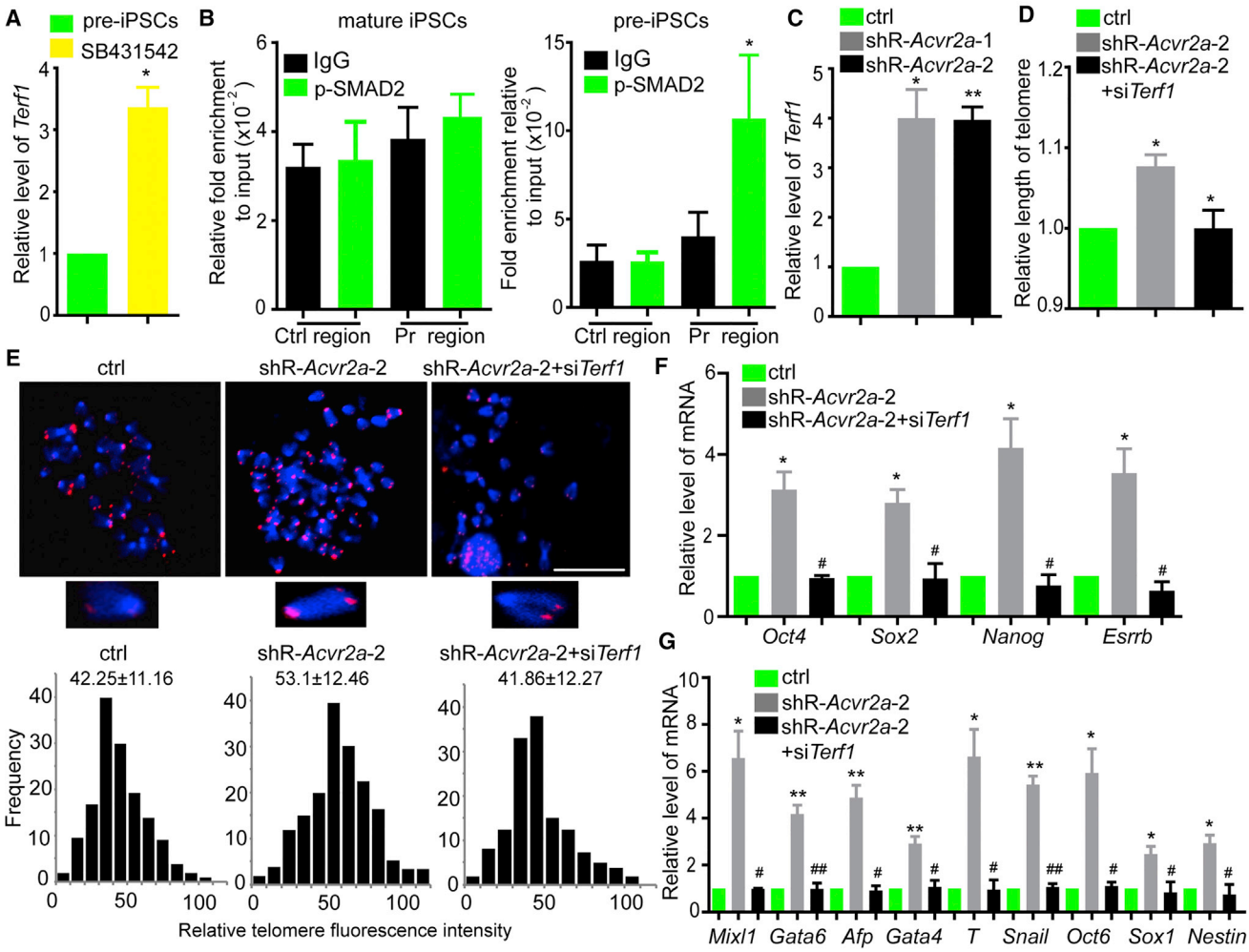

Figure 5. *Terf1* Mediates the *Acvr2a* Function in Regulating Telomere Elongation and Pluripotency

(A) Inhibition of ACTIVIN signaling by SB431542 increased *Terf1* expression. Data shown are the mean ± SD (n = 3).

(B) ChIP assays indicated that p-SMAD2 shows increased binding to the *Terf1* promoter in pre-iPSCs compared with mature iPSCs. "Ctrl region" means the sequence without p-SMAD2 binding, while "Pr region" means the prediction region of p-SMAD2 in promoter. Data shown are the mean ± SD (n = 3).

(C) Downregulation of *Acvr2a* upregulated the expression of *Terf1*. Data shown are the mean ± SD (n = 3).

(D and E) (D) Pre-iPSCs with *Terf1* knockdown blocked the increase in telomere elongation promoted by downregulation of *Acvr2a*, which was detected by both qPCR and (E) FISH assays. Scale bar indicates 10 μm. Data shown are the mean ± SD (n = 3).

(F and G) (F) Downregulation of *Terf1* prevented the function of *Acvr2a* knockdown in promoting stemness marker expression and (G) pluripotency in pre-iPSCs. Data shown are the mean ± SD (n = 3).

For all data, * and $^{\#}p < 0.05$, ** and $^{\#\#}p < 0.01$. Asterisk (*) means the statistical significance of the shR-*Acvr2a*-1 and shR-*Acvr2a*-2 group compared with the control group; hash (#) means the statistical significance of the shR-*Acvr2a*-2+si*Terf1* group compared with the shR-*Acvr2a*-2 group.

that chemical compounds (Chen et al., 2010; Li and Ding, 2010) that regulate some gene expression signaling pathways (Guo et al., 2013; Ye et al., 2012) or that promote epigenetic alteration with reprogramming factors (Huangfu et al., 2008; Shi et al., 2008) increase the quality and efficiency of iPSCs, how cells re-elongate their telomeres remains largely unknown. Our study showed that *miR-590* can target *Acvr2a* to upregulate the expression of *Terf1* and finally promote the elongation and pluripotency of pre-iPSCs.

Efficient telomere elongation is critically involved in the gain of pluripotency and is the key factor ensuring the higher quality of iPSCs (Marion et al., 2009). For ESCs, in addition to higher expression of telomerase genes and

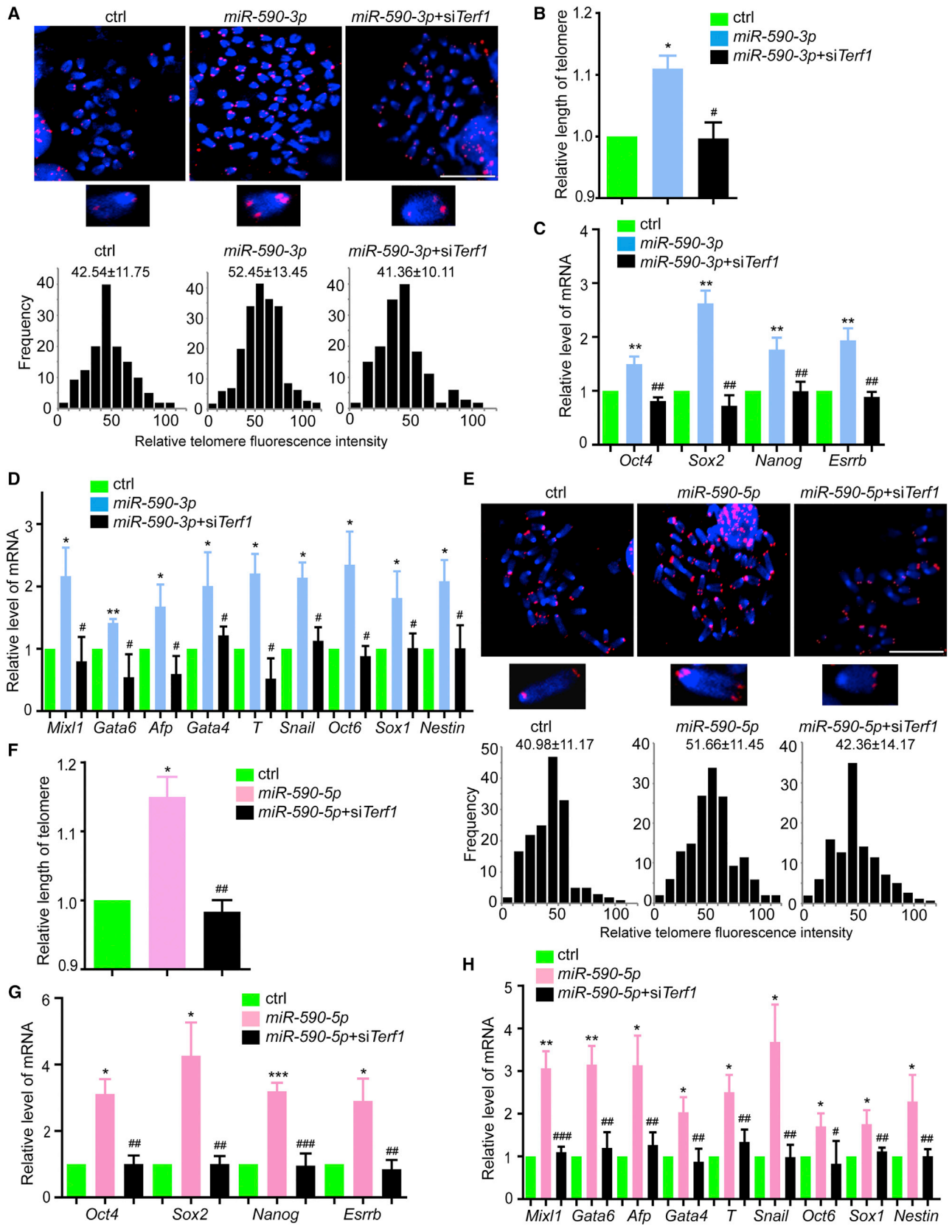

(legend on next page)

activity, *Zscan4*, which participates in the ALT process, increases the frequency of sister chromatid exchange to promote recombination (Zalzman et al., 2010). A previous study showed that *Zscan4* combined with the reprogramming factors promoted iPSC induction, quality, and telomere elongation with decreased DNA damage (Jiang et al., 2013). However, compared with the ALT process of efficient telomere elongation by utilizing SCNT (Wakayama et al., 2000), the induction of iPSCs by telomerase-dependent telomere elongation using four factors is inefficient (Le et al., 2014). In this study, we found that pre-iPSCs showed much shorter telomere lengths and lower pluripotency than ESCs or mature iPSCs. Coincidentally, *miR-590* showed higher expression in ESCs and mature iPSCs. Previous studies showed that *miR-590* increased both calcium deposition and the osteoblast differentiation marker genes' expression in mouse mesenchymal stem cells (Vishal et al., 2017). *MiR-590* could prevent the progression of aortic atherosclerosis in apolipoprotein E knockout mice (He et al., 2015). In addition, *miR-590* was also reported to be the epithelial-mesenchymal transition suppressor and downregulated in unilateral ureteral obstruction kidney mouse model (Liu et al., 2015). These studies suggested the critical roles of *miR-590* on many kinds of physiology process. Further ectopic expression of *miR-590-3p* or *miR-590-5p* in pre-iPSCs significantly promoted telomere elongation and the pluripotency of pre-iPSCs. In addition, cell reprogramming may result in abnormal chromosomes (Gore et al., 2011; Hussein et al., 2011). Our previous study indicated the role of *miR-590* in promoting DNA damage repair in mouse ESCs (mESCs) (Liu et al., 2014). These results suggested the critical function of *miR-590* during cell reprogramming by improving telomere elongation, genome stability, and cell pluripotency.

MiRNAs have been reported to be key regulators in ESCs and iPSCs and to participate in many molecular signaling pathways (Li et al., 2011; Liao et al., 2011; Samavarchi-Tehrani et al., 2010). Our previous study reported that *miR-590* directly targets *Acvr2a*, which belongs to the TGFB superfamily to enhance ESC self-renewal and DNA damage repair (Liu et al., 2014). TGFB family genes that play important roles in ESCs and iPSCs can also be regulated by miRNAs (Tan et al., 2015). It has been reported that *miR-590* directly targets *Acvr2a* to enhance ESC self-renewal and DNA damage repair (Liu et al., 2014). The *miR-302/367* cluster regulates the TGFBR2/E-CADHERIN pathway to accelerate the mesenchymal-epithelial transition process during reprogramming (Liao et al., 2011). Our study indicated that downregulation of *Acvr2a* promoted telomere elongation and pluripotency in pre-iPSCs. Rescue experiments confirmed that *Acvr2a* mediated the function of *miR-590*. These results identified the function of the TGFB family receptor gene *Acvr2a* and the *miR-590*/*Acvr2a* signaling pathway in modulating telomere elongation and reprogramming.

Telomere-related genes have been reported to be regulated by TGFB family members. Telomerase TERT can be repressed by the TGFB/p-SMAD3 pathway (Cassar et al., 2010; Wang et al., 2016). SMAD3 is recruited by OCT4 to restrict *Rif1* expression by binding to its promoter to maintain the stability of mESCs. Deletion of *Terf1* in iPSCs induced DNA damage with an increasing number of γH2AX-positive cells (Schneider et al., 2013). In MEFs, downregulation of *Terf1* inhibited cell proliferation (Martinez et al., 2009). Terf1 is important to recruit helicases to facilitate telomere lengthening (Sfeir, 2012). Previous study of the impairment of generation of iPSCs derived from the MEFs of second- and third-generation telomerase-deficient mice found that that telomeres no longer elongated and were shortening continuously during the reprogramming. In addition, although the induction efficiency of *Terc*$^{-/-}$ iPSCs derived from first-generation MEFs of telomerase-deficient mice was similar to wild-type controls, the generation of chimeric mice failed (Marion et al., 2009). Here we found that inhibition of p-SMAD2 increased the expression

Figure 6. *Terf1* Is the Functional Downstream Mediator of *miR-590* in Regulating Telomere Elongation and Pluripotency

(A) FISH assays showed that downregulation of *Terf1* blocked the improvement of telomere elongation caused by the *miR-590-3p* overexpression in the rescue experiment. Scale bar indicates 10 μm.

(B) qPCR detection of telomere length in the rescue experiment. Data shown are the mean ± SD (n = 4).

(C) Increased expression of stemness markers by *miR-590-3p* was prevented by *Terf1* knockdown. Data shown are the mean ± SD (n = 4).

(D) Detection of three germ layer markers by qPCR showed that *Terf1* downregulation blocked the improvement of pluripotency acquisition through *miR-590-3p*. Data shown are the mean ± SD (n = 3).

(E and F) (E) Downregulation of *Terf1* also blocked the *miR-590-5p* function of promoting telomere elongation as detected by both FISH and (F) qPCR. Scale bar indicates 10 μm. Data shown are the mean ± SD (n = 3).

(G and H) (G) Downregulation of *Terf1* prevented *miR-590-5p*-mediated promotion of stemness marker expression and (H) pluripotency in pre-iPSCs. Data shown are the mean ± SD (n = 3).

For all data, * and $^{\#}p < 0.05$, ** and $^{\#\#}p < 0.01$, *** and $^{\#\#\#}p < 0.001$. Asterisk (*) means the statistical significance of the *miR-590-5p* and *miR-590-3p* group compared with the control group; hash (#) means the statistical significance of the *miR-590-5p* + si*Terf1* and *miR-590-3p* + si*Terf1* group compared with the corresponding *miR-590-5p* and *miR-590-3p* group.

of *Terf1* in pre-iPSCs, elongated the telomere, and led to the maturation of pre-iPSCs. Overexpression of *Terf1* itself also promoted the telomere elongation and the maturation of pre-iPSCs. These results collectively indicated the importance of the re-elongation of short telomeres for normal iPSC generation and maturation.

Further, we determined that inhibition of ACTIVIN signaling by SB431542 or the downregulation of *Acvr2a* increased *Terf1* expression. These results suggested the function of ACTIVIN signaling in regulating *Terf1* expression. Our rescue experiments found that *Terf1* mediated the function of *Acvr2a* in regulating telomere elongation and pluripotency in pre-iPSCs. We further determined that *Terf1* is a functional downstream mediator of the *miR-590*/*Acvr2a* pathway and forms the *miR-590*/*Acvr2a*/*Terf1* axis. In addition, a previous study indicated that *Zscan4* participates in the ALT process to improve telomere elongation and the quality of iPSCs (Jiang et al., 2013). TERF1 not only interacts with ZSCAN4 but also regulates the ALT process (Lee and Gollahon, 2015). These results suggested the critical function of *Terf1* and the *miR-590*/*Acvr2a*/*Terf1* signaling pathway in improving the quality of iPSCs. Our previous study showed the *miR-590* was upregulated during the differentiation of mESCs after LIF withdrawal. *MiR-590* could regulate the expression of *Rad51b* to balance the DNA damage and cell cycle but could not influence the pluripotency of mESCs (Liu et al., 2014). Interestingly, here we found that *miR-590* was highly expressed in ESCs and iPSCs compared with pre-iPSCs. The expression of *miR-590* was also upregulated during the pre-iPSCs' maturation promoted by 2i (CHIR99021 and PD0325901). We found that inhibition of *miR-590* repressed the pluripotency acquisition of pre-iPSCs treated by 2i. This result indicated the important role of *miR-590* during the reprogramming, and the aberrant inhibition of *miR-590* expression during reprogramming might arrest the reprogramming cells in the pre-iPSC status. These findings also indicated that the regulatory mechanism of *miR-590* expression might be different during iPSC reprogramming and mESC differentiation. Our study elucidated the role of the *miR-590*/*Acvr2a*/*Terf1* signaling axis in improving telomere elongation and pluripotency of pre-iPSCs, establishing a foundation for the clinical application of iPSCs in the future.

EXPERIMENTAL PROCEDURES

Cell Culture

Mouse ESCs were cultured in 15% fetal bovine serum (FBS) (Gibco), while iPSCs and pre-iPSCs were cultured in 20% knockout serum replacement (KOSR) (Gibco) of knockout-DMEM (Gibco) medium. The medium also contained 1% nonessential amino acids (NEAAs) (Thermo), 1% mM L-glutamine (Thermo), 55 μM β-mercaptoethanol (Gibco), and LIF (Millipore). Cells were maintained on feeders at 37°C in a humidified 5% CO_2 atmosphere. The pre-iPSCs have been reported in our previous study (Wei et al., 2015).

qRT-PCR

Total RNA was isolated using RNAiso Plus (TaKaRa). cDNA synthesis from mRNA and miRNAs was performed using the cDNA Synthesis Kit (TaKaRa) and the TIANScript RT Kit (TIANGEN), respectively. The Bulge-Loop miRNA qPCR Primer Set was purchased from the RiboBio Company. Primers for the qRT-PCR analysis of mRNA are shown in Table S1.

Immunofluorescence Staining of Three Germ Layers

For the differentiation of three germ layers, cells were cultured in the medium for 48 hr, followed by withdrawing the LIF for another 7-day culture process. Medium should be changed every day. Then the differentiation cells were used for staining. First, cells were fixed with 4% paraformaldehyde (PFA) for 20 min and permeabilized with 0.2% Triton X-100 for 8 min. Cells were washed with PBS and blocked with 10% FBS (Gibco) for 1 hr at room temperature. Then, cells were stained with primary antibodies against SOX2 (Abcam, ab59776), SSEA1 (Santa Cruz, sc-101462), GATA4 (Santa Cruz, sc-9053), GATA6 (R&D Systems, AF1700), and NESTIN (Abcam, ab105389) for 12 hr at 4°C. After washing with PBS, cells were incubated with the corresponding secondary antibodies. Finally, cells were counterstained with Hoechst33342 (Sigma, 14533) to show the entire cell nucleus.

Fluorescence *In Situ* Hybridization Assay

Chromosomes were separated onto glass slides and dried overnight. Chromosomes with telomeres were denatured at 80°C for 10 min to hybridize with the red Cy3-labeled telomere peptide nucleic acid probe. Whole chromosomes were stained with 0.5 μg/mL Hoechst33342 (blue). Fluorescence of the chromosomes and telomeres was digitally imaged on a Nikon confocal laser scanning microscope with fluorescein isothiocyanate/DAPI filters. Relative telomere length was presented as telomere fluorescence intensity detected using the TFL-TELO software program.

qPCR Analysis of Relative Telomere Length

DNA of cells was isolated using a DNA isolation kit (TIANGEN). Measurements were performed as described in previous studies (Behrens et al., 2017; O'Callaghan and Fenech, 2011).

ChIP Assay

ChIP assays were performed with rabbit IgG (Cell Signaling Technology, 2729S), p-SMAD2 (Cell Signaling Technology, 3101L), POL II (Millipore, 05-263) antibodies using the ChIP assay kit (Millipore) according to the instructions. Both immunoprecipitated DNA and whole-cell DNA were used for qPCR assays of *Terf1* with the following primers: for the binding region, 5′-GAA GGGGAAGAGGGAGTGAG-3′ (forward) and 5′-TTGTCAGGCAC CTGTCTCAG-3′ (reverse); for the control region, 5′-TCAGGAAT GTCCCCTGAGAT-3′ (forward) and 5′-GCATTCCCTTCGGGTA TTTT-3′ (reverse).

RNAi Assay

For *Terf1*, the siRNA was used for RNAi by targeting the sequence GGAAGUUACUUAAGAUAAUCU (si*Terf1*) in the rescue experiments. Details of the shRNA-*Acvr2a* vectors have been reported in our previous study (Liu et al., 2014).

Statistical Analysis

The error bars represent the SD of at least three independent experiments. The statistical significance was analyzed by one-way ANOVA or Student's t test. * and $^{\#}p < 0.05$, ** and $^{\#\#}p < 0.01$, *** and $^{\#\#\#}p < 0.001$.

SUPPLEMENTAL INFORMATION

Supplemental Information includes six figures and one table and can be found with this article online at https://doi.org/10.1016/j.stemcr.2018.05.008.

AUTHOR CONTRIBUTIONS

All authors discussed the experiments and contributed to the text of the manuscript. Q.L. and G.W. designed the experiments, acquired the data, and performed the analysis. Y.L., M.B., and Z.J. contributed to plasmid construction. T.H., R.W., and Y. Yu provided materials and contributed to technical assistance. W.J. and Y. Yang discussed the project conception and design. Q.L., G.W., and J.K. conceived the project, analyzed the data, and wrote the manuscript.

ACKNOWLEDGMENTS

This work was supported by grants obtained from the Ministry of Science and Technology (2016YFA0101300), the National Natural Science Foundation of China (81530042, 31571519, 31471250, 31721003, 81600675, 31571529, 31701110, 31571390, and 31771506), the Ministry of Education (IRT_15R51), the Science and Technology Commission of Shanghai Municipality (15JC1403201), and the Fundamental Research Funds for the Central Universities (1500219106).

Received: September 26, 2017
Revised: May 16, 2018
Accepted: May 16, 2018
Published: June 14, 2018

REFERENCES

Anokye-Danso, F., Trivedi, C.M., Juhr, D., Gupta, M., Cui, Z., Tian, Y., Zhang, Y., Yang, W., Gruber, P.J., Epstein, J.A., et al. (2011). Highly efficient miRNA-mediated reprogramming of mouse and human somatic cells to pluripotency. Cell Stem Cell *8*, 376–388.

Behrens, Y.L., Thomay, K., Hagedorn, M., Ebersold, J., Henrich, L., Nustede, R., Schlegelberger, B., and Gohring, G. (2017). Comparison of different methods for telomere length measurement in whole blood and blood cell subsets: recommendations for telomere length measurement in hematological diseases. Genes Chromosomes Cancer *56*, 700–708.

Boue, S., Paramonov, I., Barrero, M.J., and Izpisua Belmonte, J.C. (2010). Analysis of human and mouse reprogramming of somatic cells to induced pluripotent stem cells. What is in the plate? PLoS One *5*, e12664.

Brambrink, T., Hochedlinger, K., Bell, G., and Jaenisch, R. (2006). ES cells derived from cloned and fertilized blastocysts are transcriptionally and functionally indistinguishable. Proc. Natl. Acad. Sci. USA *103*, 933–938.

Cassar, L., Nicholls, C., Pinto, A.R., Li, H., and Liu, J.P. (2009). Bone morphogenetic protein-7 induces telomerase inhibition, telomere shortening, breast cancer cell senescence, and death via Smad3. FASEB J. *23*, 1880–1892.

Cassar, L., Li, H., Jiang, F.X., and Liu, J.P. (2010). TGF-beta induces telomerase-dependent pancreatic tumor cell cycle arrest. Mol. Cell. Endocrinol. *320*, 97–105.

Chen, T., Yuan, D., Wei, B., Jiang, J., Kang, J., Ling, K., Gu, Y., Li, J., Xiao, L., and Pei, G. (2010). E-cadherin-mediated cell-cell contact is critical for induced pluripotent stem cell generation. Stem Cells *28*, 1315–1325.

Dahle, O., and Kuehn, M.R. (2013). Polycomb determines responses to smad2/3 signaling in embryonic stem cell differentiation and in reprogramming. Stem Cells *31*, 1488–1497.

Dinami, R., Ercolani, C., Petti, E., Piazza, S., Ciani, Y., Sestito, R., Sacconi, A., Biagioni, F., le Sage, C., Agami, R., et al. (2014). miR-155 drives telomere fragility in human breast cancer by targeting TRF1. Cancer Res. *74*, 4145–4156.

Diotti, R., and Loayza, D. (2011). Shelterin complex and associated factors at human telomeres. Nucleus *2*, 119–135.

Gore, A., Li, Z., Fung, H.L., Young, J.E., Agarwal, S., Antosiewicz-Bourget, J., Canto, I., Giorgetti, A., Israel, M.A., Kiskinis, E., et al. (2011). Somatic coding mutations in human induced pluripotent stem cells. Nature *471*, 63–67.

Guo, X., Liu, Q., Wang, G., Zhu, S., Gao, L., Hong, W., Chen, Y., Wu, M., Liu, H., Jiang, C., et al. (2013). microRNA-29b is a novel mediator of Sox2 function in the regulation of somatic cell reprogramming. Cell Res. *23*, 142–156.

He, P.P., OuYang, X.P., Li, Y., Lv, Y.C., Wang, Z.B., Yao, F., Xie, W., Tan, Y.L., Li, L., Zhang, M., et al. (2015). MicroRNA-590 inhibits lipoprotein lipase expression and prevents atherosclerosis in apoE knockout mice. PLoS One *10*, e0138788.

Ho, A., Wilson, F.R., Peragine, S.L., Jeyanthan, K., Mitchell, T.R., and Zhu, X.D. (2016). TRF1 phosphorylation on T271 modulates telomerase-dependent telomere length maintenance as well as the formation of ALT-associated PML bodies. Sci. Rep. *6*, 36913.

Huang, J., Wang, F., Okuka, M., Liu, N., Ji, G., Ye, X., Zuo, B., Li, M., Liang, P., Ge, W.W., et al. (2011). Association of telomere length with authentic pluripotency of ES/iPS cells. Cell Res. *21*, 779–792.

Huangfu, D., Osafune, K., Maehr, R., Guo, W., Eijkelenboom, A., Chen, S., Muhlestein, W., and Melton, D.A. (2008). Induction of pluripotent stem cells from primary human fibroblasts with only Oct4 and Sox2. Nat. Biotechnol. *26*, 1269–1275.

Hussein, S.M., Batada, N.N., Vuoristo, S., Ching, R.W., Autio, R., Narva, E., Ng, S., Sourour, M., Hamalainen, R., Olsson, C., et al. (2011). Copy number variation and selection during reprogramming to pluripotency. Nature *471*, 58–62.

Ichida, J.K., Blanchard, J., Lam, K., Son, E.Y., Chung, J.E., Egli, D., Loh, K.M., Carter, A.C., Di Giorgio, F.P., Koszka, K., et al. (2009). A small-molecule inhibitor of tgf-Beta signaling replaces sox2 in reprogramming by inducing nanog. Cell Stem Cell *5*, 491–503.

Jiang, J., Lv, W., Ye, X., Wang, L., Zhang, M., Yang, H., Okuka, M., Zhou, C., Zhang, X., Liu, L., et al. (2013). Zscan4 promotes genomic stability during reprogramming and dramatically improves the quality of iPS cells as demonstrated by tetraploid complementation. Cell Res. *23*, 92–106.

Lanza, R.P., Cibelli, J.B., Diaz, F., Moraes, C.T., Farin, P.W., Farin, C.E., Hammer, C.J., West, M.D., and Damiani, P. (2000). Cloning of an endangered species (*Bos gaurus*) using interspecies nuclear transfer. Cloning *2*, 79–90.

Le, R., Kou, Z., Jiang, Y., Li, M., Huang, B., Liu, W., Li, H., Kou, X., He, W., Rudolph, K.L., et al. (2014). Enhanced telomere rejuvenation in pluripotent cells reprogrammed via nuclear transfer relative to induced pluripotent stem cells. Cell Stem Cell *14*, 27–39.

Lee, K., and Gollahon, L.S. (2015). ZSCAN4 and TRF1: a functionally indirect interaction in cancer cells independent of telomerase activity. Biochem. Biophys. Res. Commun. *466*, 644–649.

Li, W., and Ding, S. (2010). Small molecules that modulate embryonic stem cell fate and somatic cell reprogramming. Trends Pharmacol. Sci. *31*, 36–45.

Li, Z., Yang, C.S., Nakashima, K., and Rana, T.M. (2011). Small RNA-mediated regulation of iPS cell generation. EMBO J. *30*, 823–834.

Liao, B., Bao, X., Liu, L., Feng, S., Zovoilis, A., Liu, W., Xue, Y., Cai, J., Guo, X., Qin, B., et al. (2011). MicroRNA cluster 302-367 enhances somatic cell reprogramming by accelerating a mesenchymal-to-epithelial transition. J. Biol. Chem. *286*, 17359–17364.

Liu, L., Bailey, S.M., Okuka, M., Munoz, P., Li, C., Zhou, L., Wu, C., Czerwiec, E., Sandler, L., Seyfang, A., et al. (2007). Telomere lengthening early in development. Nat. Cell Biol. *9*, 1436–1441.

Liu, Q., Wang, G., Chen, Y., Li, G., Yang, D., and Kang, J. (2014). A miR-590/Acvr2a/Rad51b axis regulates DNA damage repair during mESC proliferation. Stem Cell Rep. *3*, 1103–1117.

Liu, T., Nie, F., Yang, X., Wang, X., Yuan, Y., Lv, Z., Zhou, L., Peng, R., Ni, D., Gu, Y., et al. (2015). MicroRNA-590 is an EMT-suppressive microRNA involved in the TGFbeta signaling pathway. Mol. Med. Rep. *12*, 7403–7411.

Luo, Z., Feng, X., Wang, H., Xu, W., Zhao, Y., Ma, W., Jiang, S., Liu, D., Huang, J., and Songyang, Z. (2015). Mir-23a induces telomere dysfunction and cellular senescence by inhibiting TRF2 expression. Aging Cell *14*, 391–399.

Marion, R.M., Strati, K., Li, H., Tejera, A., Schoeftner, S., Ortega, S., Serrano, M., and Blasco, M.A. (2009). Telomeres acquire embryonic stem cell characteristics in induced pluripotent stem cells. Cell Stem Cell *4*, 141–154.

Martinez, P., Thanasoula, M., Munoz, P., Liao, C., Tejera, A., McNees, C., Flores, J.M., Fernandez-Capetillo, O., Tarsounas, M., and Blasco, M.A. (2009). Increased telomere fragility and fusions resulting from TRF1 deficiency lead to degenerative pathologies and increased cancer in mice. Genes Dev. *23*, 2060–2075.

O'Callaghan, N.J., and Fenech, M. (2011). A quantitative PCR method for measuring absolute telomere length. Biol. Proced. Online *13*, 3.

Pera, M.F. (2011). Stem cells: the dark side of induced pluripotency. Nature *471*, 46–47.

Samavarchi-Tehrani, P., Golipour, A., David, L., Sung, H.K., Beyer, T.A., Datti, A., Woltjen, K., Nagy, A., and Wrana, J.L. (2010). Functional genomics reveals a BMP-driven mesenchymal-to-epithelial transition in the initiation of somatic cell reprogramming. Cell Stem Cell *7*, 64–77.

Schneider, R.P., Garrobo, I., Foronda, M., Palacios, J.A., Marion, R.M., Flores, I., Ortega, S., and Blasco, M.A. (2013). TRF1 is a stem cell marker and is essential for the generation of induced pluripotent stem cells. Nat. Commun. *4*, 1946.

Sfeir, A. (2012). Telomeres at a glance. J. Cell Sci. *125*, 4173–4178.

Shi, Y., Do, J.T., Desponts, C., Hahm, H.S., Scholer, H.R., and Ding, S. (2008). A combined chemical and genetic approach for the generation of induced pluripotent stem cells. Cell Stem Cell *2*, 525–528.

Silva, J., Barrandon, O., Nichols, J., Kawaguchi, J., Theunissen, T.W., and Smith, A. (2008). Promotion of reprogramming to ground state pluripotency by signal inhibition. PLoS Biol. *6*, e253.

Stadtfeld, M., and Hochedlinger, K. (2010). Induced pluripotency: history, mechanisms, and applications. Genes Dev. *24*, 2239–2263.

Takahashi, K., and Yamanaka, S. (2006). Induction of pluripotent stem cells from mouse embryonic and adult fibroblast cultures by defined factors. Cell *126*, 663–676.

Tan, F., Qian, C., Tang, K., Abd-Allah, S.M., and Jing, N. (2015). Inhibition of transforming growth factor beta (TGF-beta) signaling can substitute for Oct4 protein in reprogramming and maintain pluripotency. J. Biol. Chem. *290*, 4500–4511.

Theunissen, T.W., van Oosten, A.L., Castelo-Branco, G., Hall, J., Smith, A., and Silva, J.C. (2011). Nanog overcomes reprogramming barriers and induces pluripotency in minimal conditions. Curr. Biol. *21*, 65–71.

Vishal, M., Vimalraj, S., Ajeetha, R., Gokulnath, M., Keerthana, R., He, Z., Partridge, N.C., and Selvamurugan, N. (2017). MicroRNA-590-5p stabilizes Runx2 by targeting Smad7 during osteoblast differentiation. J. Cell. Physiol. *232*, 371–380.

Wakayama, T., Tateno, H., Mombaerts, P., and Yanagimachi, R. (2000). Nuclear transfer into mouse zygotes. Nat. Genet. *24*, 108–109.

Wakayama, S., Jakt, M.L., Suzuki, M., Araki, R., Hikichi, T., Kishigami, S., Ohta, H., Van Thuan, N., Mizutani, E., Sakaide, Y., et al. (2006). Equivalency of nuclear transfer-derived embryonic stem cells to those derived from fertilized mouse blastocysts. Stem Cells *24*, 2023–2033.

Wang, X.H., Liu, M.N., Sun, X., Xu, C.H., Liu, J., Chen, J., Xu, R.L., and Li, B.X. (2016). TGF-beta1 pathway affects the protein expression of many signaling pathways, markers of liver cancer stem cells, cytokeratins, and TERT in liver cancer HepG2 cells. Tumour Biol. *37*, 3675–3681.

Wei, T., Chen, W., Wang, X., Zhang, M., Chen, J., Zhu, S., Chen, L., Yang, D., Wang, G., Jia, W., et al. (2015). An HDAC2-TET1 switch at

distinct chromatin regions significantly promotes the maturation of pre-iPS to iPS cells. Nucleic Acids Res. *43*, 5409–5422.

Xin, H., Liu, D., and Songyang, Z. (2008). The telosome/shelterin complex and its functions. Genome Biol. *9*, 232.

Yang, X., Smith, S.L., Tian, X.C., Lewin, H.A., Renard, J.P., and Wakayama, T. (2007). Nuclear reprogramming of cloned embryos and its implications for therapeutic cloning. Nat. Genet. *39*, 295–302.

Ye, D., Wang, G., Liu, Y., Huang, W., Wu, M., Zhu, S., Jia, W., Deng, A.M., Liu, H., and Kang, J. (2012). MiR-138 promotes induced pluripotent stem cell generation through the regulation of the p53 signaling. Stem Cells *30*, 1645–1654.

Zalzman, M., Falco, G., Sharova, L.V., Nishiyama, A., Thomas, M., Lee, S.L., Stagg, C.A., Hoang, H.G., Yang, H.T., Indig, F.E., et al. (2010). Zscan4 regulates telomere elongation and genomic stability in ES cells. Nature *464*, 858–863.

Zhao, X.Y., Li, W., Lv, Z., Liu, L., Tong, M., Hai, T., Hao, J., Guo, C.L., Ma, Q.W., Wang, L., et al. (2009). iPS cells produce viable mice through tetraploid complementation. Nature *461*, 86–90.